

Article citation info:

Meng Z, Ma C, Xie Y, Influence of impact load form on dynamic response of chock-shield support, *Eksploracja i Niezawodność – Maintenance and Reliability* 2023; 25(3) <http://doi.org/10.17531/ein/168316>

Influence of impact load form on dynamic response of chock-shield support

Indexed by:



Zhaosheng Meng^a, Chen Ma^a, Yunyue Xie^{a,*}

^a Shandong University of Science and Technology, China

Highlights

- Mechanical-Hydraulic co-simulation model is developed for chock-shield support.
- The influence of different loading forms on the reliability of the support is analyzed.
- The joint that may reduce the reliability of the support is obtained.
- The load at each joint of the support is typically non-uniformity.

Abstract

Chock-shield support is usually used in underground coal mining to protect the roof. However, as the mining depth gets deeper, impact load that came from the roof becomes stronger and more frequent. This causes the support to bear a large number of dynamic loads, and reducing its reliability. To improve the support performance of the chock-shield support, the mixed-kinetic model was established using the mechanical-hydraulic co-simulation method. The load distribution law of the support joint under impact load form different stability forces, impact load amplitude, and impact frequency is discussed. The mechanical-hydraulic cooperative response of the chock-shield support are obtained. The results show that different joints show typical non-uniformity characteristic during the loading process. The proposed mechanical-hydraulic co-simulation method can more accurately obtain the dangerous points of hydraulic support reliability. The results of this study will help to improve the reliability of the chock-shield support.

Keywords

hydraulic support, dynamic load, reliability analysis, mechanical-hydraulic co-simulation

This is an open access article under the CC BY license (<https://creativecommons.org/licenses/by/4.0/>)

1. Introduction

With the rapid and stable growth of China's economic transformation, the mining and utilization of the coal resource are accelerated. As the key supporting equipment for coal mining, chock-shield support has been more and more widely used to protect the roof [3,9,16,18]. During the mining process, the top beam of the chock-shield support is in contact with the roof plate and the base plate is in contact with the bottom plate. The roof plate, bottom plate and the coal seam together form the "strata system". The function of the support is to help prevent the subsidence of roof strata and ensures the mining face working normally. As the working face advances, the roof plate

behind the support canopy will cave randomly or periodically, forming an impact load on the support. The released impact energy caused by the roof plate caving reaches up to 10^6 - 10^8 J [14,15]. When the impact load appears, key structural components such as the hinge points, top beam plates will undergo significant deformation. This reduces the support stability of the support and poses a threat to the safety of workers. Therefore, the reliable operation of the supports is an important prerequisite for ensuring the safe production of the working face. In recent years, the shallow buried coal resources are gradually exhausted, and people have had to mine deeper

(*) Corresponding author

E-mail addresses: Z. Meng (ORCID: 0000-0002-8103-694X) skdmzs@163.com, C. Ma (ORCID: 0000-0002-4179-7381) m863425381@163.com, Y. Xie (ORCID: 0000-0003-2313-2922) xieyunyue515@sdust.edu.cn,

coal. Meanwhile the mining height of the working face is also getting higher. These all cause the support to bear a large number of dynamic loads and reducing its reliability [8,12,22,27].

Since the support equipment has an important influence on safe mining. Many scholars have done lots works to improve the performance of the support. By establishing a mechanical model of two-column shield support, Wang et al. [19] introduced the impact coefficient to describe the adaptability of the joint to impact load. Wo et al. [21] analyzed the rule of support strength change on roof settlement characteristics. He points out that stronger support strength will be beneficial to roof settlement control. By using the Finite Element Method analysis method and applying horizontal and bending load to the support, He et al. [6] studied the stress distribution law of the top beam and determined the dangerous area that may lead to the support failure. By modelling a hydraulic support simulation model and applying a uniform load to the top beam position, Li et al. [10] obtained the stress nephogram of the support under different loads and proposed a structural optimization plan for the support. To analyze the load distribution rule of the two-column shield support, Zeng et al. [25,26] built the mechanical model of the support and applied the impact load to different position on the support. According to the D'Alembert principle, Guan et al [5] established a multi-degree-of-freedom numerical analysis model of the hydraulic support and modified the front linkage structure. Then he compared the operating characteristics of the hydraulic cylinder and found that the improved structural components could further ensure the safe operation of the hydraulic support. Liang et al. [11] proposed an impact dynamics model considering the flexible jack system of the hydraulic brace. He applied impact loads to different locations of the top beam and analyzed the force transfer law of each articulation point of the brace. Hu et al. [7] developed a mechanical structure model of hydraulic bracket lifting stability based on D'Alembert's principle. Then he analyzed the influence of different support heights, different lifting speeds, and other factors on bracket lifting stability performance with the help of numerical calculation methods. The existing research has focused on the impact of changes in impact load position on the dynamic response of two-column support, and less on the impact of different impact load forms

on the dynamic response of four-column chock-shield support. The existing research generally only involves mechanical system or hydraulic system, without considering the synergy of these two factors. To obtain the performance of chock-shield support under different impact loads more comprehensively, it is necessary to establish a mechanical-hydraulic collaborative simulation (MHC) model. The method of co-simulation analysis used in this paper is more applied in the research fields of automobile and robotics [4,13,23,28], which can cut down the production process, reduce the cost and improve the accuracy of simulation analysis in the practical application process. However, this method is less applied in the direction of hydraulic support.

Based on the previous studies, to further discuss the dynamic response of the chock-shield support under different load impact modes. The ZZ18000/33/72D type chock-shield support was chosen in this study, the MHC characteristics of the support was taken into account, and the mixed-kinetic model of the support was created. The influence of changes in setting force, impact load amplitude and impact frequency on the response differences of the support was compared based on the established model. The load transfer law of hinge joints at different positions is finally obtained. This paper will be helpful for the reliability design and analysis of the chock-shield support.

2. Establishment of the MHC model

2.1 The mechanical system model

In this study, the ZZ18000/33/72D type chock-shield support is chosen, the specific parameters of the support are shown in Table 1. The “ZZ18000/33/72D” is the product code of the selected support. The “ZZ” represents a four-column chock-shield support, the “18000” represents the rated working resistance of the support (18000 kN), the “33/72” indicates that the minimum and maximum working height of the support is 3300 mm and 7200 mm, respectively. The “D” represents that the support is electro-hydraulic controlled. The ADAMS software is selected to establish the mechanical system model. The connecting mode of the columns are defined as moving pair constraints and that of the others parts are rotating pair constraints. The selected support is equipped with double telescopic columns. To establish the force, speed and

displacement transmission interface between the mechanical system and hydraulic system, Marker points are set at the center of the piston cylinder and piston rod, respectively. The force variables are defined as Input variables (input from hydraulic system to mechanical system), the speed and displacement variables are defined as Output variables (output from mechanical system to hydraulic system). Fig. 1 shows the established mechanical model of the ZZ18000/33/72D support.

Table 1 Main parameters of the ZZ18000/33/72D support

Items	value
Operation height(mm)	3300~7200
Centerline spacing (mm)	1750
Width(mm)	1680~1880
Setting force (kN)	12977
Working force (kN)	18000
Support strength (MPa)	1.73~1.78
The top beam length (mm)	6200
The shield beam length (mm)	4527
The front rod length (mm)	3710
The rear rod length (mm)	3445

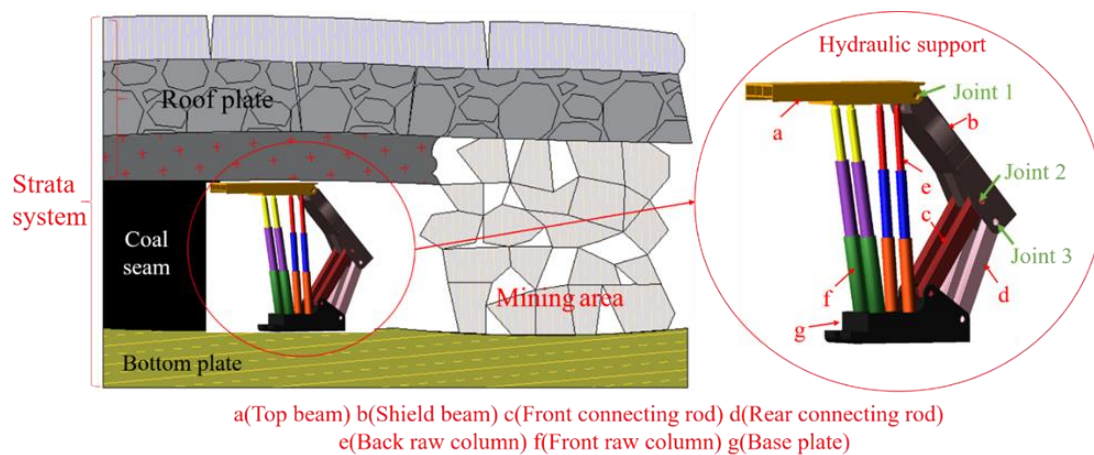


Figure 1. Mechanical system model of the support.

2.2 The hydraulic system model

The hydraulic support studied in this paper contains four columns. For the convenience of narration, it is named the front

raw column (FRC) and the back raw column (BRC) according to the spatial position of the column. Figure 2 shows the defined hydraulic system model.

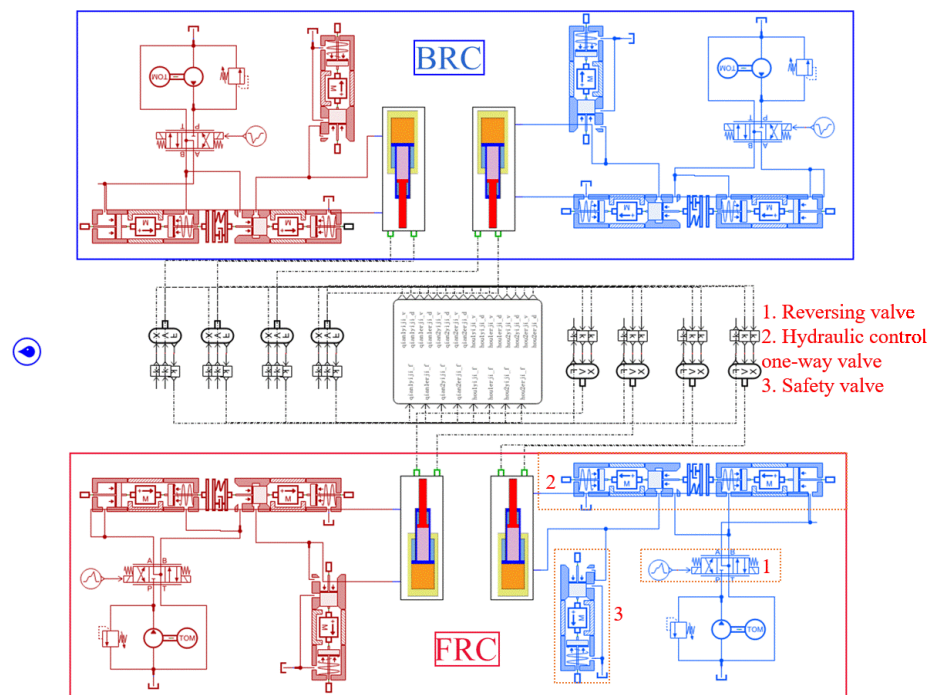


Figure 2. Hydraulic system model of the support.

Then the column system models at different positions are established, respectively. It mainly includes hydraulic control one-way valve, safety valve, and other directional and pressure control elements as well as the double telescopic column. The components are established by using the Hydraulic Components

Design (HCD) library in AMESim and the reliability test is carried out. After the test is qualified, the above single components are combined into a complete hydraulic system model. The key dimensions of the double telescopic columns are listed in Table 2.

Table 2. Key dimensions for the column system.

Items		External diameter (mm)	Internal diameter (mm)	Setting force (kN)	Working force (kN)
The front raw column(FRC)	First stage	400	380	3956	5489
	Second stage	290	260		
The back raw column(BRC)	First stage	320	290	2532	3513
	Second stage	230	210		

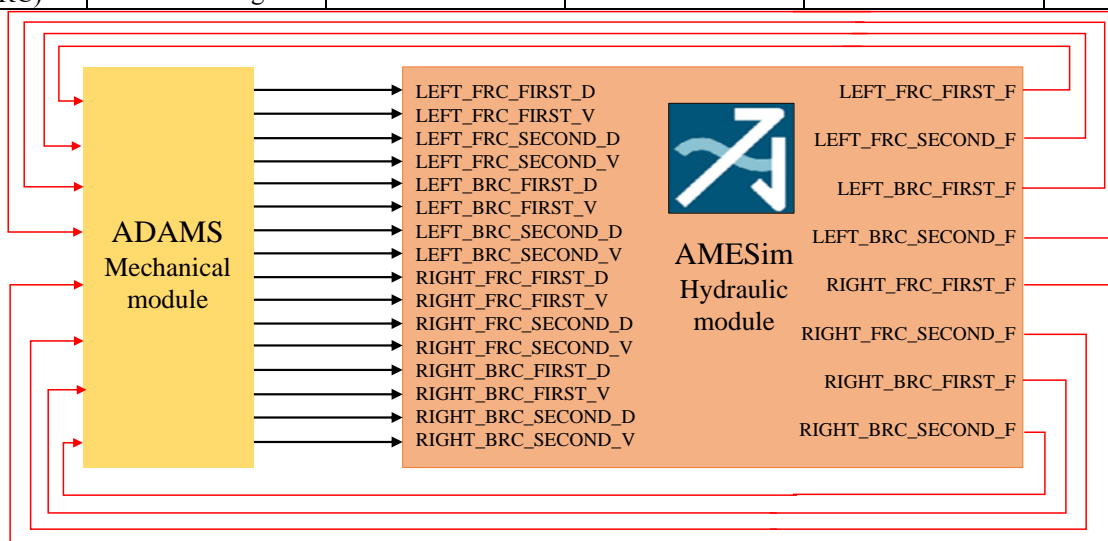


Figure 3. The MHC model of the support.

The established mechanical system and hydraulic system models are imported into MATLAB, respectively. The data interaction interface between ADAMS and AMESim is established using MATLAB/Simulink. Fig.3 shows the established MHC model of the chock-shield support. In the figure, the “LEFT” means the left column, the “FIRST” means the first stage, the “D”, “V” and “F” means the displacement, velocity and force variable, respectively. In the mechanical system model, the animation mode is interactive, the simulation step is 0.0001 s, and the compilation language is C++. In the hydraulic model, the simulation step is 0.0001 s, and the variable function is ode45 (Fourth-Fifth order Runge-Kutta algorithm).

equipment, the support bears the stability force and impact force from the roof at the same time. The roof is connected by collision contact to transfer the upper load to the support. In this section, a setting force (14000 kN) is applied to the roof directly in 4 s to check the stability of the support. Figure 4 shows the loading form of the support (the impact loading is not activated here).

3. Stability analysis of the MHC model

3.1 The load application mode

During the mining process, the support, rock strata and coal seam are always in dynamic balance state. As the main support

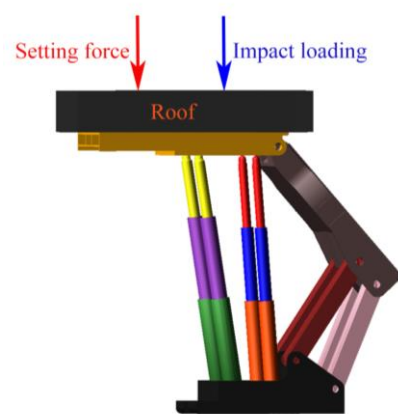


Figure 4. The loading form of the support.

3.2 Stability test of the MHC model

Figure 5 shows the results of model stability analysis. As can be seen, the force acting on the top beam reaches 14000 kN in about 4 seconds and then remains unchanged. The pressure and support force of the columns also reach the peak value at this time. The pressure of the FRC and BRC is stabilized at 32 MPa (4043 kN) and 43 MPa (3537 kN), respectively. As the external force grows gradually, the columns are also pressurized

gradually. Since the cylinder diameter of the FRC is larger than that of the BRC, even if the forces applied to columns are equal, the column pressure still shows a large difference. Through the cooperation of the connecting joint, the structural parts at different positions of the support are built into a complete mechanical structure. Therefore, the mutual movement of the structural parts changes the load at the joint. With the change of the bearing state and the supporting force, the load at joint 1 (See Fig.1) finally stabilizes at 897 kN.

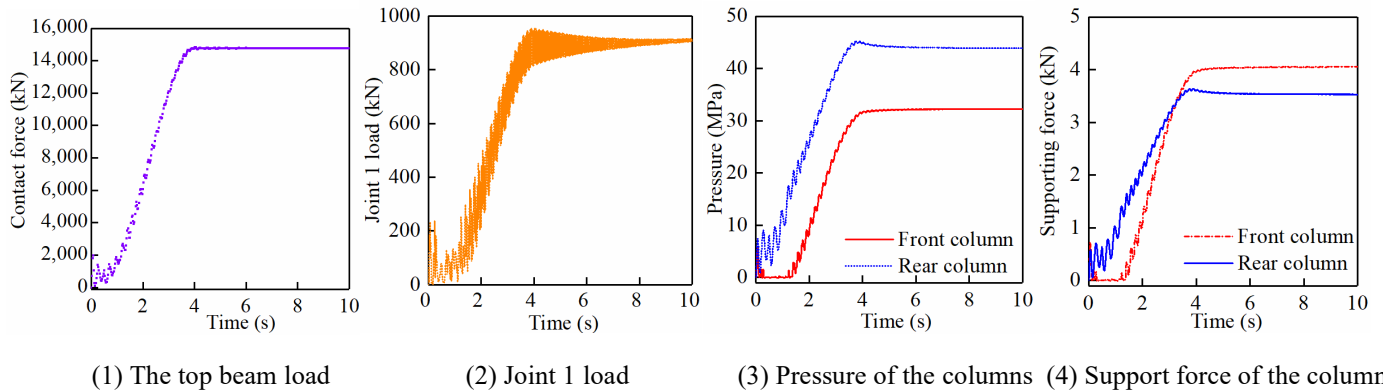


Figure 5. Partial stability test results of the MHC model.

4. Result analysis of the support in different load form

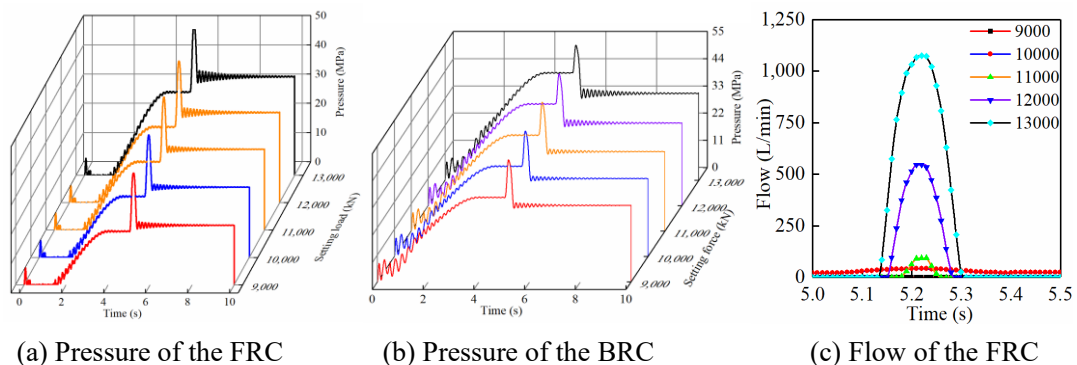
4.1 Influence of the setting force

During the operation cycle, the support will form different steady support forces on the roof due to the loss along the way and unloading of safety valve [1,2]. To test the response difference of support under different setting forces, the setting forces of 9000 kN ~13000 kN is selected (every 1000 kN). The impact load is fixed as 7000 kN, the action time of the setting force is 5 s, the impact load action time is 0.2 s, and the whole simulating time is 10 seconds.

(1) Dynamic response of the column system

The reactions of the column system with the same impact load and different setting forces is shown in Fig.6. During the

setting force loading process, the stable pressure of the FRC increased from 18.3 MPa (2269 kN) to 28.7 MPa (3587 kN). The stable pressure of the BRC increased from 34.3 MPa (2747 kN) to 43.4 MPa (3501 kN). It can be observed that before the impact loading appears, the load borne by the FRC increases gradually (from 45.2% to 50%) with the setting force. At the time the impact load appears, the peak supporting force of the FRC increased from 4797 kN to 6431 kN, the peak supporting force of the BRC increased from 3975 kN to 4404 kN, and the load borne by the front row increased by 4.4% (from 54.6% to 59%). With the increase of the stability force before the impact load, the load distribution ratio of the FRC and BRC has changed. The load bearing ratio of the front row columns has increased significantly (up to about 5%).



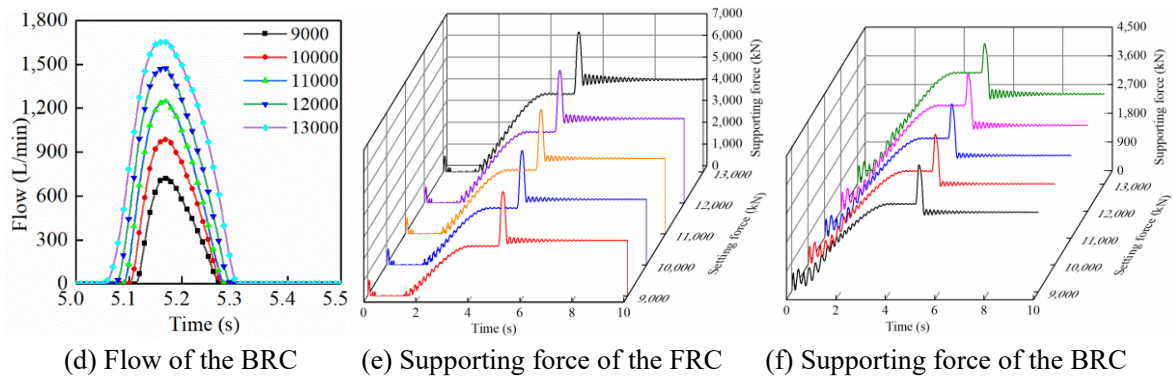


Figure 6: Dynamic response of the support in different setting force.

Comparing the flow curve of the rodless cavity of the front and BRC with different stability forces, it can be seen that the FRC not reach the switching pressure of the relief valve when the setting force is 9000 kN. The cylinder diameter of the BRC is smaller than that of the FRC, the BRC reaches the opening pressure under the same load. Therefore, there is no overflow in the FRC, and the safety valve of the BRC has reached the opening pressure.

(2) Dynamic response of the joints

The existing studies show that the joints, as the key connection structure, is the most vulnerable part of the support. Therefore, studying and improving the load distribution law of the joints is helpful to improve the reliability of the support [18,24]. Figure 7 depicts the joints load variation at different locations in the mechanical structure. It can be remarked that before the impact loading appears, the load of joints at different positions has basically stabilized under the given setting force. When the stable load is 13000 kN, the maximum load of joint 1, 2, 3 (See Fig.1) is 858 kN, 4060 kN, and 3600 kN, the

corresponding minimum load is 531 kN, 2408 kN, and 2172 kN. It can be seen that joint 2 has the largest LIR of 1.69, while joint 1 is the about 1.61. When the impact loading appears, as the setting force grows, the peak load curve (1367 kN) of joint 1 reached at 5.2 s, the peak load of joint 2 at this time was 6451 kN, and the peak load of joint 3 was 5727 kN. It can be seen that at the moment of impact, the stress of structural members at different positions is uneven, and the load of joint 2 is the largest (4.7 times of joint 1). It is important to pay attention to whether there are dangerous situations such as stress concentration in the working process.

When the impact load appears, with the increase of stability force, joint 1 reaches the peak value of 1367 kN at 5.2 s. While the peak value of joint 2 and joint 3 reaches 5727 kN at this time. It can be found that the stresses in the structural members at different locations of the hydraulic support show obvious non-uniformity under the impact loading. The load of joint 2 is the largest (4.7 times than that of joint 1). Obviously, joint 2 is easier to reduce support reliability.

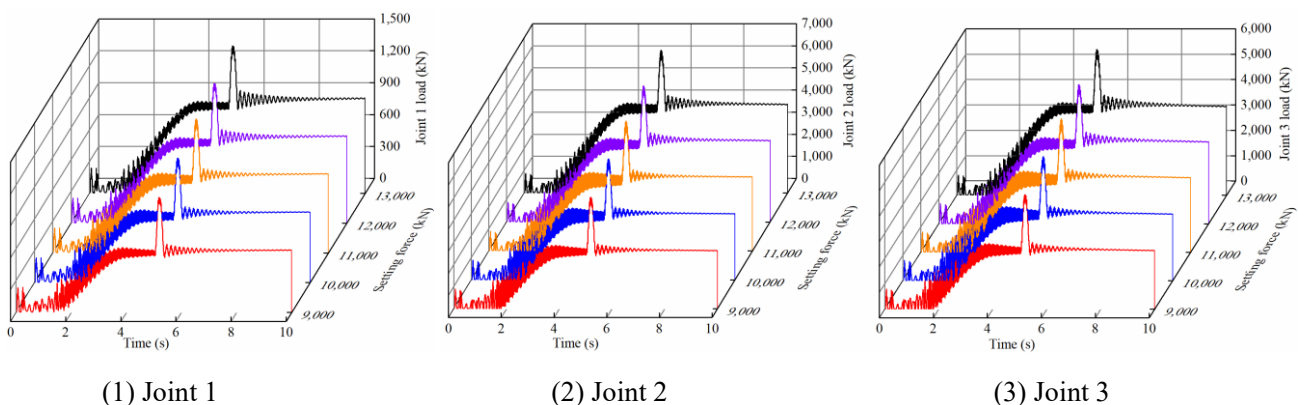


Figure 7. Joints load under different initial setting force.

4.2 Influence of the impact load amplitude

To further study the effect of impact loading variation on the dynamic response of support under the same setting force, this

section fixes the setting force at 11000 kN. By changing the amplitude of impact load (5000 kN ~9000 kN, increments 1000 kN), the load transfer performance of support with different

impact forces is compared [17,20].

(1) Dynamic response difference of the column system

Figure 8 shows the reaction of the column system for different impact loading amplitudes. The pressure, flow and supporting force response of the column rodless cavity are essentially the same because the set force is fixed before the impact loading appears. The peak pressure in the rodless cavity of the FRC increases to 51.1 MPa from 38.3 MPa, and the peak pressure in the BRC increases to 55.2 MPa from 49.2 MPa after the impact loading occurred. After the impact loading disappears, the performance of the columns is basically the same, from the peak value to the stable value gradually. As the impact loading grows, the peak supporting force of BRC increased from 3961 kN to 4450 kN (the LIR is about 1.13), while the peak value of the FRC supporting force increased

from 4814 kN to 6424 kN (the LIR is about 1.34). The FRC replaces the BRC as the main bearing capacity structural member. At this stage, the FRC also bears more load than the BRC. Therefore, by increasing the diameter of the FRC, the load acting point can be moved forward to better control the front roof.

The FRC does not reach the switching pressure of the relief valve when the impact load is 5000 kN and 6000 kN. The cylinder diameter of the BRC is smaller than that of the FRC. At this time, the BRC is easier to reach the switching overflow pressure of the relief valve. Then, with the further increase of the impact loading, the front and BRC s can reach the switching pressure of the relief valve. The overflow from the BRC through the relief valve is the largest. The maximum flow is about 1700 L/min and appears at 5.17 s.

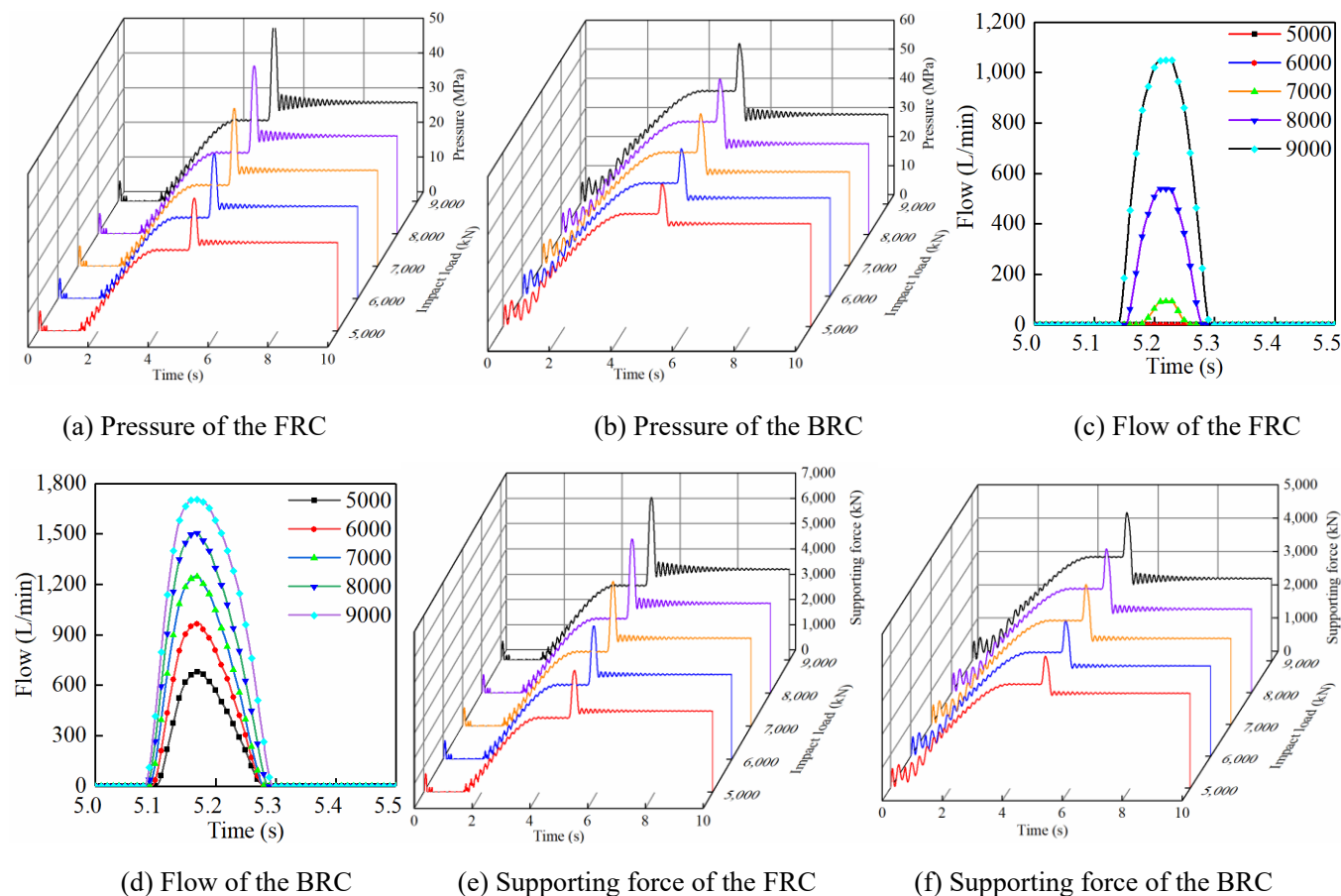


Figure 8. Dynamic response of the support under different impact load.

(2) Dynamic response of the joints

Figure 9 displays the dynamic response of the joints under differing impact loading. When the impact load appears, the joints load increases and reaches the peak value rapidly. When the impact loading is 9000 kN, the load of joint 1, 2, and 3 is

1385 kN, 6534 kN, and 5815 kN, respectively. Compared with the impact load of 5000 kN, the maximum LIR of the joints is 1.28 and it appears at joint 2. Therefore, the joint 2 has higher probability reducing the reliability of the support.

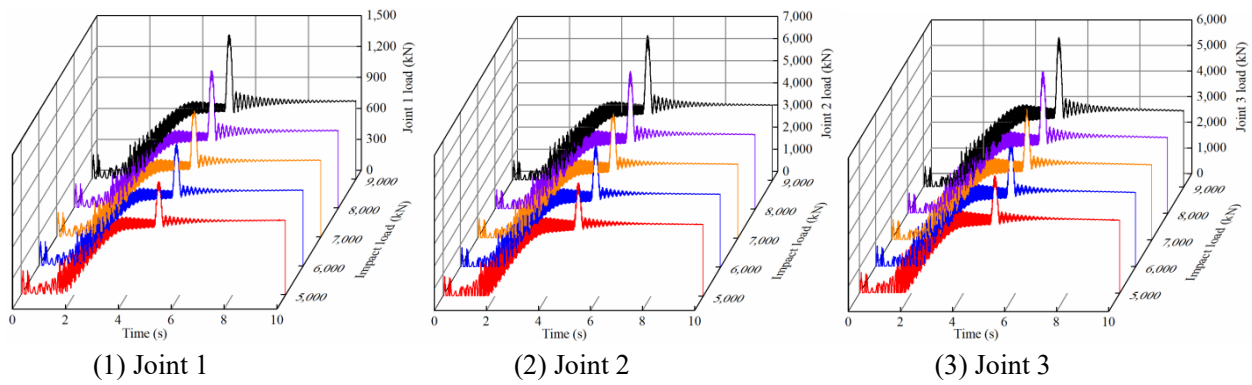


Figure 9. Joints load under different impact load.

4.3 Influence of the impact frequency

When the support reaches the rated operation height, it forms an elastic coupling with the roof. Therefore, the hydraulic support is vulnerable to multiple impacts of roof load in the support process. To analyze the response difference of the support when multiple impact loads appear, different numbers of triangular impact loads are selected in this section. The time interval of the impact load is 0.2 s. The setting force and the impact load is defined as is 11000 kN and 7000 kN, respectively. The impact frequency of the impact load is 1, 2, 3, 4 and 5, respectively.

(1) Dynamic response difference of the column system

Figure 10 indicates the response of the column system under different impact loading frequency. As can be seen, with the increase of the impact frequency, multiple pressure peaks appear in the columns. The peak pressure of the FRC increased

from 45.4 MPa to 48.6 MPa, and the supporting force increased from 5715 kN to 6116 kN. Since the LIR of the columns changes during the impact process, the FRC bear more load than the BRC. When the BRC system is loaded, the peak value of the pressure and supporting force decreases gradually. The peak pressure and supporting force of the BRC decreases from 52.1 MPa to 45.8 MPa, and from 4201 kN to 3847 kN. By comparing the rodless cavity of the columns, it can be noted that with the increase of the impact frequency, the peak pressure in the rodless cavity of the FRC shows an ascendant trend. This is because the front and BRC have different proportion of load distribution. When the impact loading works on the support firstly, the load and flow (1245 L/min) of the BRC reaches the maximum. Then, as the increase of the load frequency, the peak overflow of the BRC shows a decreasing trend.

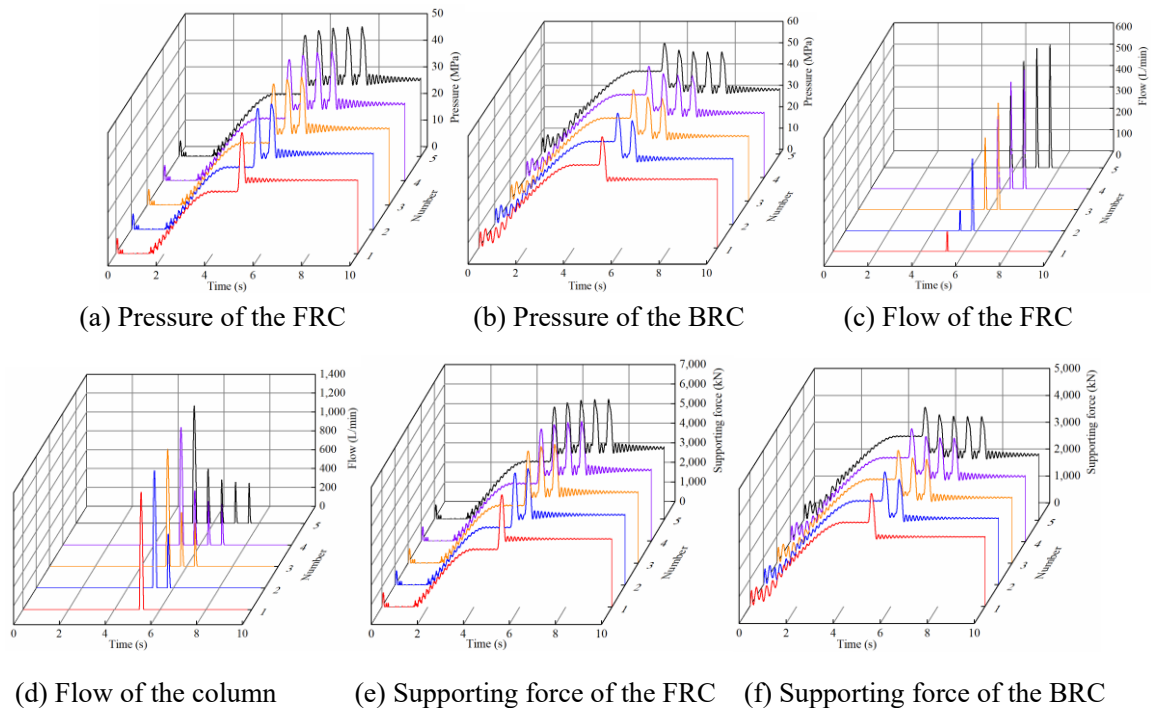


Figure 10: Dynamic response of support under different impact frequency.

(2) Dynamic response of the joints

Figure 11 indicates the load variation of the joint at different impact frequencies. It can be seen that with the growth of the impact frequency, the loading of the joints shows multiple peaks when the impact load appears. The peak load of joint 2, joint 3 and joint 1 is basically stable at 5800 kN, 5200 kN and 1260 kN, respectively. Then, with the disappearance of the impact

load, the load of joints decreases gradually and finally becomes stable. The impact frequency does not change the trend after the joint load is stabilized. The stable load of joint 1, joint 2, joint 3 is 770 kN, 3370 kN and 2920 kN, respectively. The joints load at different positions do not show obvious variation law with the increase of the impact frequency.

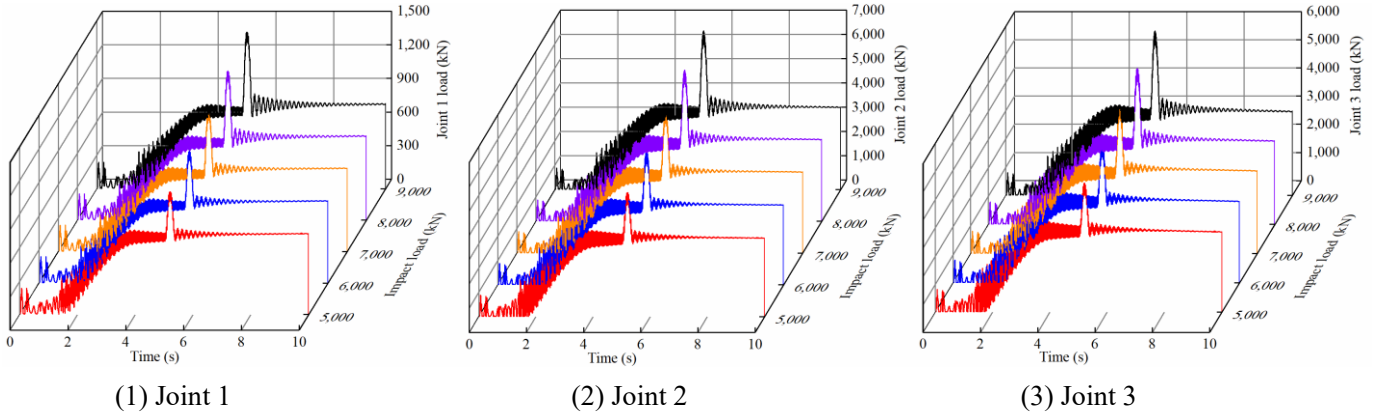


Figure 11. Joints load under different impact frequency.

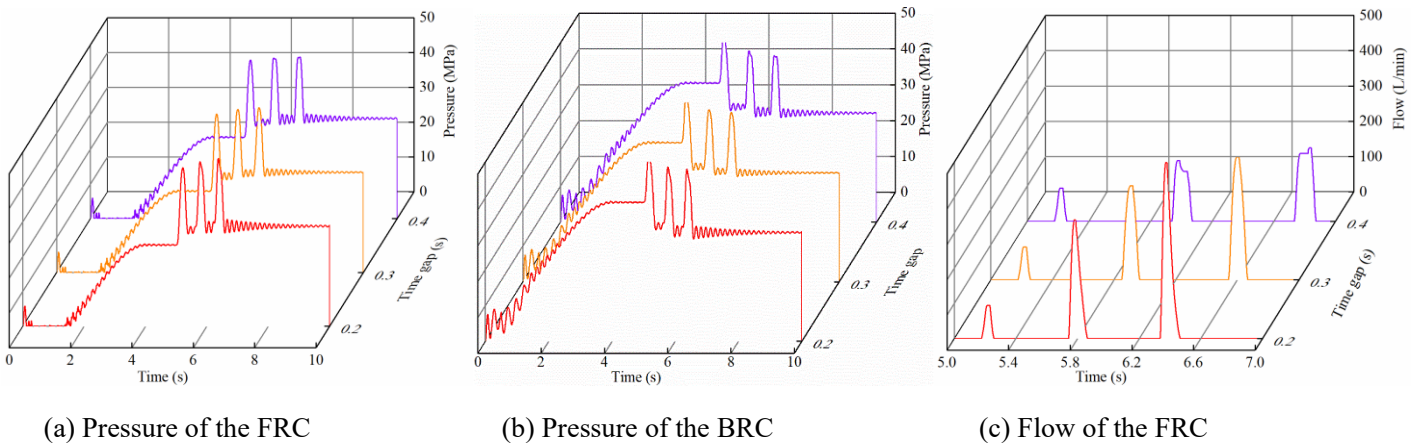
4.4. Influence of impact time gaps

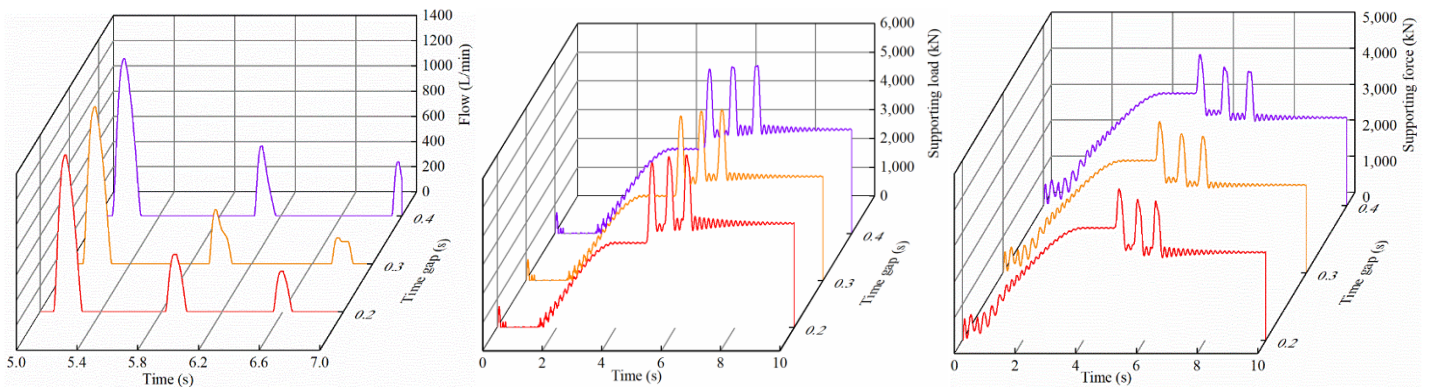
The relative movement of the hydraulic support and the roof is prone to generate complex loads, the load time interval may change due to the disorder of load. To understand the effect of impact interval on the dynamic reaction of the support, the impact frequency, initial setting force, impact load and time gap of the support is defined as 3, 11000 kN, 7000 kN and 0.2 s to 0.4 s, respectively.

(1) Dynamic response difference of the column system

Figure 12 notes the variations of the column system in different time gaps. As the time gaps increase, the fluctuation

transition of the pressure curve at the peak value is gradually smooth, and the third peak value of the front and BRC decreases from 48.2 MPa to 46.2 MPa, and from 47.9 MPa to 46.1 MPa (with a decrease of about 2 MPa), respectively. It can be noted that the third peak load of the FRC and BRC decreased from 6061 kN to 5806 kN, and from 3864 kN to 3710 kN. The overflow of the front and BRC also shows a decreasing trend. Because the impact time gap increases, the column system has enough recovery time to the original state. Therefore, when multiple impact loads act on the support, the sensitivity of the hydraulic support to abrupt loading decreases as the time gaps increase.





(d) Flow of the BRC

(e) Supporting force of the FRC

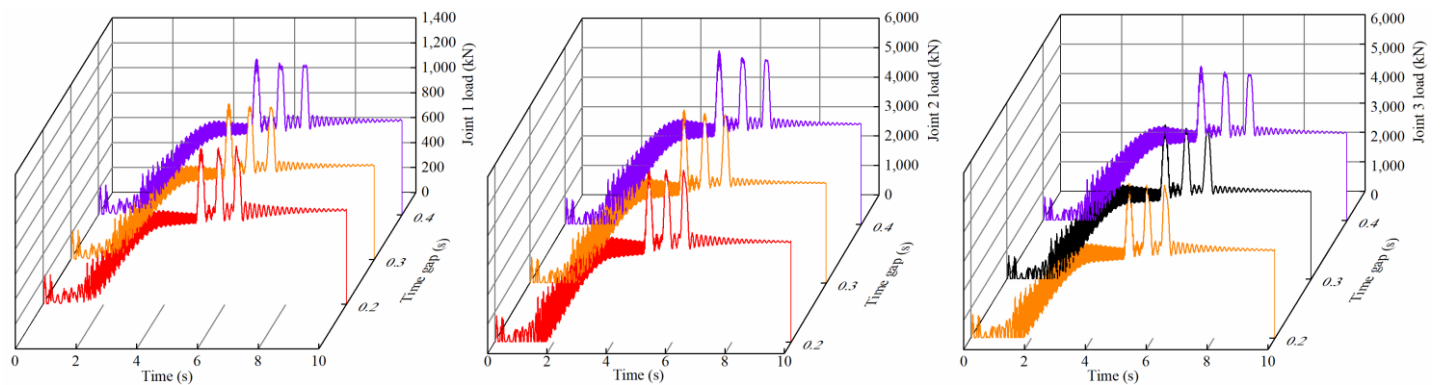
(f) Supporting force of the BRC

Figure 12. Dynamic response of support under different impact gaps.

(2) Dynamic response of the joints

Figure 13 shows the joint load under different impact time gaps. Increasing time gaps gives more response time to the support system. The peak loads of the joints also show a tendency to decrease. Therefore, the increase in impact time

results in an enhanced carrying capacity of the support in response to load impact. However, by comparing the peak joint load, it can be noted that the impact time gaps do not have a significant influence on the joint load.



(1) Joint 1

(2) Joint 2

(3) Joint 3

Figure 13. Joints load under different impact time gaps.

5. Conclusions

To research the effect of impact loading on the operational reliability of the chock-shield support working reliability, this paper takes ZZ18000/33/72D type support as the research object. After building the MHC model, the dynamic change differences of the support under different forms of impact loading is analyzed. The main results are shown below:

(1) The MHC analysis model of the support is established, and the rationality is tested by applying setting force to the model. In the stability test stage, the supporting force of the FRC increases gradually with the stability force (about 1.14 times of the BRC). When the impact loading is fixed, the joint load shows typical non-uniformity with the increase of the stability force.

(2) As the impact loading increases, The FRC shows a larger LIR (about 1.34) than that of the BRC (only about 1.13). Compared to others joints, the joint 2 shows a continuous high additional load characteristic. During the mining process, the cylinder diameter ratio of the front and BRC can be appropriately increased to enhance the reliability of the support.

(3) Compared with the single impact loading, the load response of the columns varies greatly with the impact loading frequency. The peaks of pressure and supporting force of the FRC and the joints all show an increasing trend, making a load of joint 2 increase to the maximum (about 5800 kN). During the design process, the load state of joint 2 must be closely observed to prevent the support from premature failure.

(4) With the increase of impact interval, the peak load of the

support is significantly reduced. Therefore, additional energy-absorbing structures can be considered to reduce the impact frequency of the hydraulic support, so as to improve the reliability of the support.

To study the effect of varying forms of loading on the impact reliability of the support, an ideal MHC model is developed in

this paper. Due to the calculation time and efficiency, the influence of the joint clearance is not considered. To improve the accuracy of the results, further consideration will be given to the effect of clearance position and size on the operational reliability of the chock-shield support.

Acknowledgements

This research was funded by the National Natural Science Foundation of China (52104164, 52274132) and the Natural Science Foundation of Shandong Province (ZR2020QE103), Central government guidance for local projects (YDZX2022013).

References

1. Cao LM, Xu GT, Su GX, Cao HL. Design of automatic pressurizing device of hydraulic support initial force. *Energy Science & Engineering* 2020,8(8). doi:10.1002/ese3.705.
2. Cao LM, Zhang F, Chen WY, Chen LJ. Design and Analysis on a Pressure Control Device to Setting Load for Hydraulic Support in Coal Face. *The Open Mechanical Engineering Journal* 2015,9(1). doi:10.2174/1874155x01509010124.
3. Chen NN, Fang XQ, Liang MF, Xue XM, Zhang F, Wu G, Qiao FK. Research on Hydraulic Support Attitude Monitoring Method Merging FBG Sensing Technology and AdaBoost Algorithm. *Sustainability* 2023, 15(3). doi:10.3390/SU15032239.
4. Duyun Tatyana, Duyun Ivan, Rybak Larisa, Perevuznik Victoria. Simulation of the structural and force parameters of a robotic platform using co-simulation. *Procedia Computer Science* 2022, 213. doi:10.1016/J.PROCS.2022.11.126.
5. Guan EG, Miao HH, Li PB, Zhao YZ. Dynamic model analysis of hydraulic support. *Advances in Mechanical Engineering* 2019, 11(1). doi:10.1177/1687814018820143.
6. He WB, Chen ZJ, Du JG, Yao HY. Finite Element Analysis of Combination Condition of ZF6400/19/32 Hydraulic Support. *IOP Conference Series: Materials Science and Engineering* 2019, 490(5). doi:10.1088/1757-899X/490/5/052006.
7. Hu XP, Liu XH. Stability analysis of four-column hydraulic support. *Journal of Vibration and Shock* 2021, 40(19):1-11+25. <https://doi.org/10.1155/2021/5547222>.
8. Jiao XB, Xie JC, Wang XW, Yan ZW, Hao ZX, Wang XS. Intelligent decision method for the position and attitude self-adjustment of hydraulic support groups driven by a digital twin system. *Measurement* 2022, 202. doi:10.1016/J.MEASUREMENT.2022.111722.
9. Li JW, Fu BJ, Zhang HL, Zhao QC, Bu QW. Study on Fracture Behavior of Directly Covered Thick Hard Roof Based on Bearing Capacity of Supports. *Applied Sciences* 2023, 13(4):2546. doi:10.3390/APP13042546.
10. Li TD, Wang JR, Zhang K, Zhang CH. Mechanical analysis of the structure of longwall mining hydraulic support. *Science Progress* 2020, 103(3). doi:10.1177/0036850420936479.
11. Liang LC, Tian JJ, Zheng H, Jiao SJ. A study on force transmission in a hydraulic support under impact loading on its canopy beam. *Journal of China Coal Society* 2015, 40(11):2522-2527. doi:10.13225/j.cnki.jccs.2015.7021.
12. Lin JZ, Yang TR, Ni KX, Han CY, Ma H, Gao A, Xiao CL. Effects of boundary conditions on stress distribution of hydraulic support: A simulation and experimental study. *Advances in Mechanical Engineering* 2021, 13(3). doi:10.1177/16878140211001194.
13. Nagarajan P, Vigneshwaran S, Yuvaraj K, Mohammed Ismail A, Raghavendra Prabhu S. Modelling of Robotic Single Peg-In-Hole Assembly Using ADAMS/MATLAB Co-simulation. *IOP Conference Series: Materials Science and Engineering* 2020, 995(1). doi:10.1088/1757-899X/995/1/012008.
14. Pan YS, Qi QX, Wang AW, Xiao YH, Chen JQ, Lu XF, et al. Theory and technology of three levels support in bump-prone road way. *Journal of China Coal Society* 2020, 45(5). doi:10.13225/j.cnki.jccs.DY20.0261.
15. Pan YS, Song YM, Zhu CL, Ren H, Xu HL. Localization method of coal rock deformation for rock burst prediction. *Journal of China Coal Society* 2023,48(1). doi:10.13225/j.cnki.jccs.2022.1375.
16. Pang YH, Wang HB, Lou JF, Chai HL. Longwall face roof disaster prediction algorithm based on data model driving. *International Journal of Coal Science & Technology* 2009, (1). doi:10.1007/S40789-022-00474-4.

17. Ren HW, Zhang DS, Gong SX, Zhou K, Xi CY, He M, Li TJ. Dynamic impact experiment and response characteristics analysis for 1:2 reduced-scale model of hydraulic support. *International Journal of Mining Science and Technology* 2021,31(3). doi:10.1016/J.IJMST.2021.03.004.
18. Wan LR, Jiang K, Zeng QL, Gao KD. Dynamic response and reliability analysis of shearer drum cutting performance in coal mining process. *Eksploatacja i niezawodność - maintenance and reliability* 2022,24(1). doi:10.17531/EIN.2022.1.14.
19. Wang DL, Zeng XT, Wang GF, Li R. Adaptability Analysis of Four-Column Hydraulic Support with Large Mining Height under Impact Dynamic Load. *Shock and Vibration* 2022, 2022. doi:10.1155/2022/2168871.
20. Wang XW, Gui T, Xie JC, Shen HD, Liu Ym, WBB. Virtual simulation method of hydraulic support motion considering pin shaft clearance. *Coal Science and Technology* 2021,49(2) : 186-193. doi: 10. 13199/j. cnki. cst. 2021. 02. 022
21. Wo XF, Li GC, Li JH, Yang S, Lu ZC, Hao HR, Sun YT. The Roof Safety under Large Mining Height Working Face: A Numerical and Theoretical Study. *Minerals* 2022, 12(10). doi:10.3390/MIN12101217.
22. Yang XJ, Wang RF, Wang HF, Yang YK. A novel method for measuring pose of hydraulic supports relative to inspection robot using LiDAR. *Measurement* 2020, 154(C). doi:10.1016/j.measurement.2019.107452.
23. Yang YL, Wang JR, Shi LW, Li J. Gait Simulation Research of 2-DOF Lower Limb Rehabilitation Robot Based on ADAMS and MATLAB. *Journal of Physics: Conference Series* 2022, 2414(1). doi:10.1088/1742-6596/2414/1/012020.
24. Yang Z K, Sun ZY, Jiang SB, Xu CZ. Structural Analysis on Impact-Mechanical Properties of Ultra-High Hydraulic Support. *International Journal of Simulation Modeling* 2020,19(1). doi:10.2507/IJSIMM19-1-498.
25. Zeng QL, Li ZJ, Wan LR, Ma DJ, Wang JT. Research on Dynamic Characteristics of Canopy and Column of Hydraulic Support under Impact Load. *Energies* 2022, 15(13). doi:10.3390/EN15134638.
26. [26] Zeng QL, Xu PH, Meng ZS, Ma C, Lei XW. Posture and Dynamics Analysis of Hydraulic Support with Joint Clearance under Impact Load. *Machines* 2023, 11(2). doi:10.3390/MACHINES11020159.
27. Zhang K, Li YX, Feng L, Meng XJ, Zhong DH, Huang LS. Roof deformation characteristics and experimental verification of advanced coupling support system supporting roadway. *Energy Science & Engineering* 2022, 10(7). doi:10.1002/ESE3.1145.
28. Zhang XW, Liang HB, Wang XH, Li Q. Integrated Direct Yaw Control and Antislip Regulation Mixed Control of Distributed Drive Electric Vehicle Using Cosimulation Methodology. *Mathematical Problems in Engineering* 2022, 2022. doi:10.1155/2022/6749649.